Electronic Supplementary Information

Layered cobalt oxide epitaxial films exhibiting thermoelectric ZT = 0.11 at room temperature

Yugo Takashima,[a] Yu-qiao Zhang,*[b] Jiake Wei,[c,d] Bin Feng,[c] Yuichi Ikuhara,[c,d] Hai Jun Cho,[a,b] and Hiromichi Ohta*[a,b]

Author affiliations

* Corresponding authors

[a]Graduate School of Information Science and Technology, Hokkaido University, N14W9, Kita, Sapporo 060−0814, Japan

[b]Research Institute for Electronic Science, Hokkaido University, N20W10, Kita, Sapporo 001−0020, Japan

E-mail: yuqiaozhang0730@gmail.com

E-mail: hiromichi.ohta@es.hokudai.ac.jp

[c]Institute of Engineering Innovation, The University of Tokyo, 2−11−16 Yayoi, Bunkyo, Tokyo 113−8656, Japan

[d]Elements Strategy Initiative for Structural Materials, Kyoto University, Yoshida-honmachi, Sakyo-ku, Kyoto 606−8501, Japan

Table S1. Thermoelectric properties of the layered cobaltite epitaxial films in the in-plane direction at room temperature. In addition to the observed properties, we calculated the lattice thermal conductivity ($\kappa_{lattice} = \kappa_{obsd} - \kappa_{electron}$). The electron thermal conductivity ($\kappa_{electron}$) was estimated by assuming the Wiedemann-Franz law ($\kappa_{electron} = L \cdot \sigma \cdot T$, where the L is 2.44×10^{-8} W Ω K^{-2}).

	$Ca_{1/3}CoO_2$ [19]	$Na_{0.75}CoO_2$	$Sr_{1/3}CoO_2$ [21]	$Ba_{0.27}CoO_2$
σ_{in} (S cm^{-1})	1330	1330	890	2310
S_{in} (μV K^{-1})	+90	+96	+115	+72
PF_{in} (mW m^{-1} K^{-2})	1.08	1.23	1.18	1.20
$\kappa_{in\ obsd}$ (W m^{-1} K^{-1})	6.79	5.46	4.51	3.29
$\kappa_{in\ electron}$ (W m^{-1} K^{-1})	0.98	0.97	0.65	1.69
$\kappa_{in\ lattice}$ (W m^{-1} K^{-1})	5.81	4.49	3.86	1.60
ZT_{in}	0.048	0.067	0.078	0.11

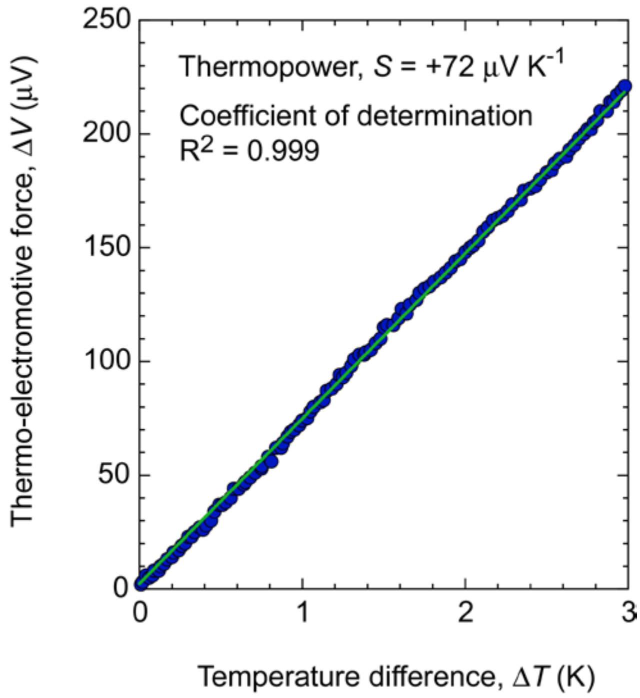

Figure S1. Typical thermo-electromotive force (ΔV) vs. temperature difference (ΔT) plot of the resultant $Ba_{0.27}CoO_2$ epitaxial film at room temperature. The thermopower (S) was calculated to be +72 μV K^{-1} as the linear slope of the ΔT – ΔV plot. The coefficient of determination (R^2) was 0.999.

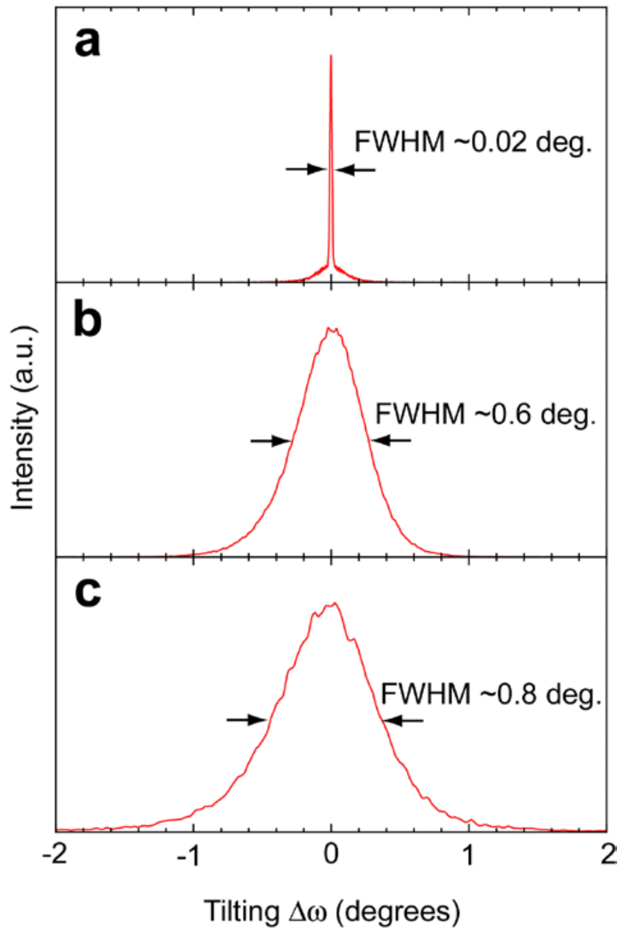

Figure S2. Average crystal tilting of the resultant films in the out-of-plane direction. Out-of-plane X-ray rocking curves of (a) 111 CoO after step 1, (b) 0002 $Na_{0.75}CoO_2$ after step 2, and (c) 0002 $Ba_{1/3}CoO_2$ after step 3. The full-width at half maximum (FWHM) values are (a) ~0.02°, (b) ~0.6° and (c) ~0.8°, respectively. Since the topographic AFM images of these films [Figs. 3(d)−(f)] show grain growth tendency, the increasing tendency of the FWHM values reflects the warp of the films, not mosaicity.

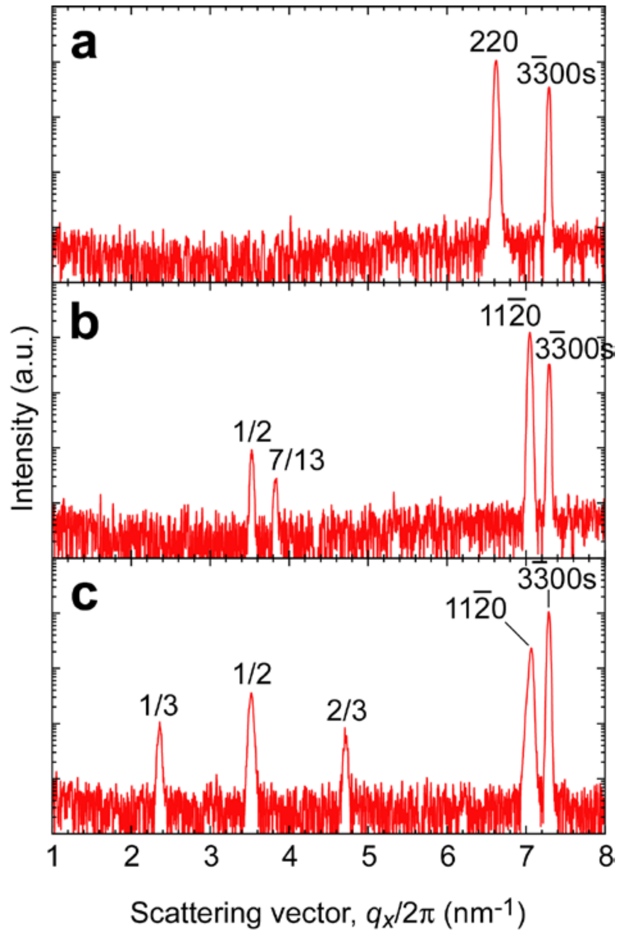

Figure S3. Change in the in-plane XRD pattern of the resultant films on (0001) α-Al_2O_3 substrate. (a) After step 1 (CoO), (b) after step 2 ($Na_{0.75}CoO_2$), and (c) after step 3 ($Ba_{1/3}CoO_2$). The epitaxial relationship of (a) is (111)[110] CoO || (0001)[1-100] α-Al_2O_3, (b) is (0001)[1-120] $Na_{0.75}CoO_2$ || (0001)[1-100] α-Al_2O_3, and (c) is (0001)[1-120] $Ba_{1/3}CoO_2$) || (0001)[1-100] α-Al_2O_3, respectively. Several diffraction peaks due to sublattices of Na (1/2 and 7/13) and Ba (1/3, 1/2, and 2/3) are clearly seen in (b) and (c).

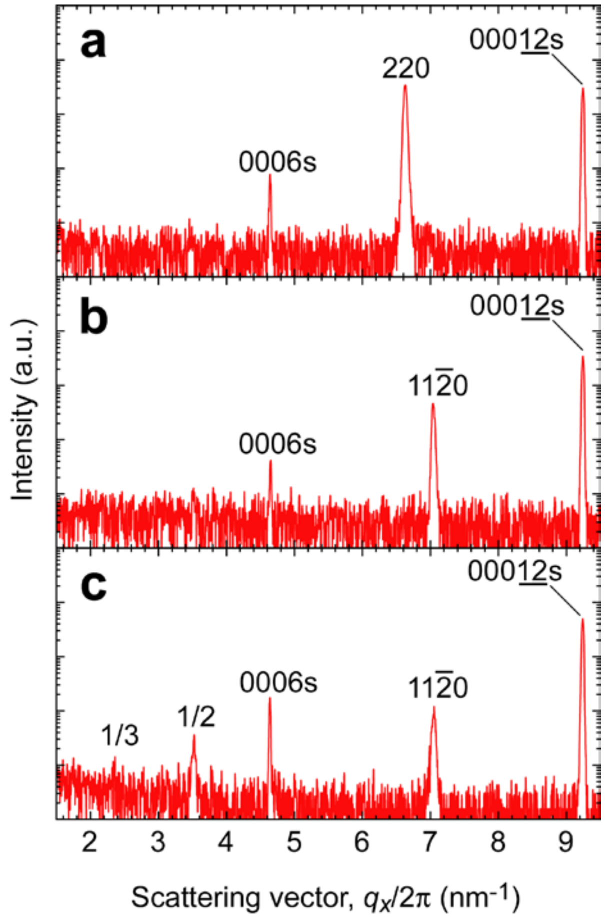

Figure S4. Change in the in-plane XRD pattern of the resultant films on (1-100) α-Al_2O_3 substrate. (a) After step 1 (CoO), (b) after step 2 ($Na_{0.75}CoO_2$), and (c) after step 3 ($Ba_{1/3}CoO_2$). The epitaxial relationship of (a) is [110] CoO || [0001] α-Al_2O_3, (b) is [1-120] $Na_{0.75}CoO_2$) || [0001] α-Al_2O_3, and (c) is [1-120] $Ba_{1/3}CoO_2$ || [0001] α-Al_2O_3, respectively. Several diffraction peaks due to sublattices of Ba (1/3 and 1/2) are clearly seen in (c).

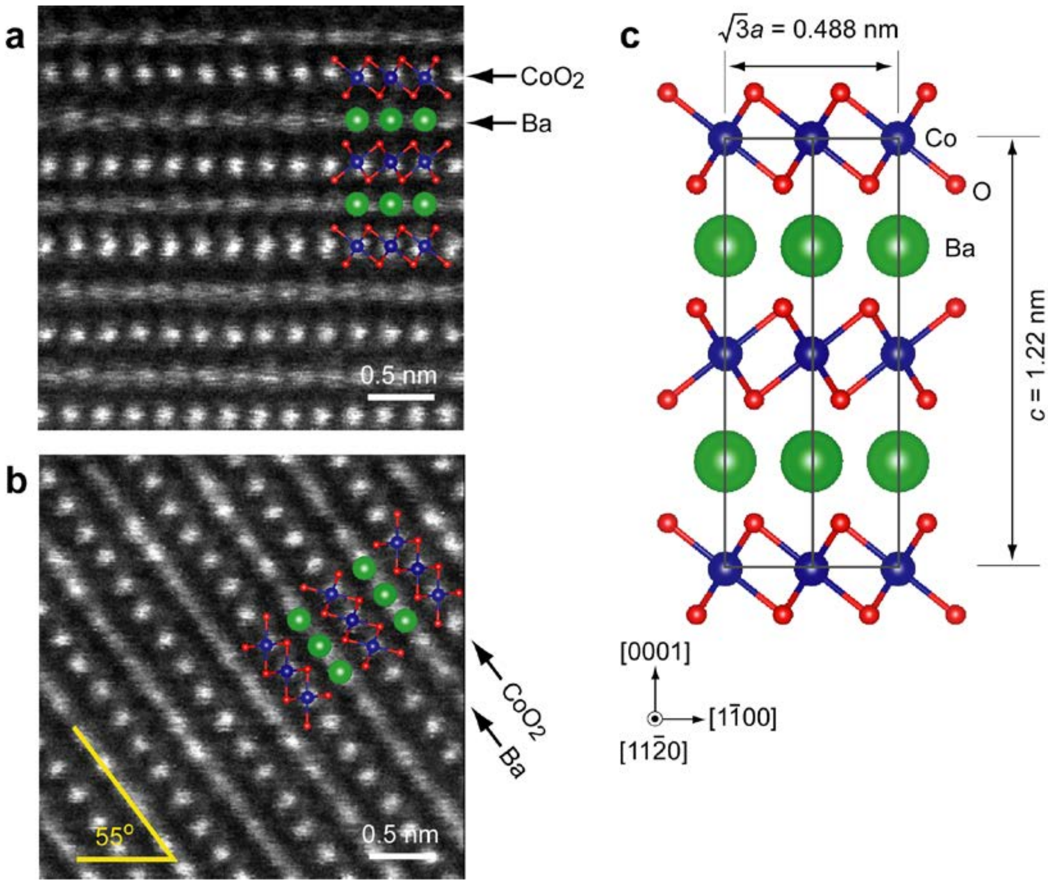

Figure S5. The atomic arrangement of the $Ba_{0.27}CoO_2$ films. The magnified HAADF-STEM image of the film grown on (a) (0001) α-Al_2O_3 substrate and (b) (1-100) α-Al_2O_3 substrate. The schematic crystal structure of $Ba_{1/3}CoO_2$ (c) is superimposed in the STEM images. The Ba and CoO_2 layers are stacked parallel to the (0001) substrate surface whereas Ba and CoO_2 layers are inclined 55° to the (1-100) substrate surface.

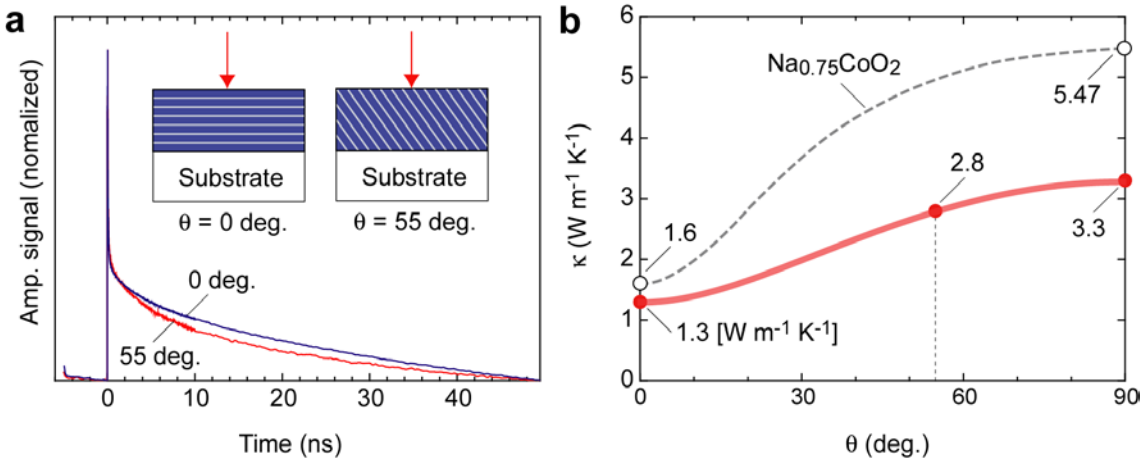

Figure S6. Thermal conductivity of the $Ba_{0.27}CoO_2$ epitaxial films at room temperature. (a) Decay curves of TDTR signal. The 55° inclined film shows faster decay. (b) Thermal conductivity of the $Ba_{0.27}CoO_2$ epitaxial films. The observed thermal conductivity of the *c*-axis oriented $Ba_{0.27}CoO_2$ epitaxial film ($\theta = 0°$) was 1.3 W m^{-1} K^{-1} and that of the 55° inclined film was 2.8 W m^{-1} K^{-1}. The thermal conductivity along the CoO_2 layer ($\theta = 90°$) was obtained theoretically using these values.